THE JOURNAL OF PHYSICAL CHEMISTRY A

Article

pubs.acs.org/JPCA

On the Role of Nonspherical Cavities in Short Length-Scale Density Fluctuations in Water

Gabriele Cesare Sosso,*[,†] Sebastiano Caravati,[‡] Grant Rotskoff,[§] Suriyanarayan Vaikuntanathan,[∥] and Ali Hassanali*[,⊥]

[†]Thomas Young Centre, London Centre for Nanotechnology and Department of Physics and Astronomy, University College London, Gower Street, London WC1E 6BT, United Kingdom

[‡]Department of Chemistry, University of Zurich, Winterhurerstrasse 190, Zurich CH-8057, Switzerland

[§]Biophysics Graduate Group, University of California, Berkeley, California 94720, United States

[∥]Department of Chemistry, The University of Chicago, Chicago, Illinois 60637, United States

[⊥]Condensed Matter and Statistical Physics Section, The Abdus Salam International Centre for Theoretical Physics, I-34151 Trieste, Italy

Supporting Information

ABSTRACT: Density fluctuations in liquid water are at the heart of numerous phenomena associated with hydrophobic effects such as protein folding and the interaction between biomolecules. One of the most fundamental processes in this regard is the solvation of hydrophobic solutes in water. The vast majority of theoretical and numerical studies examine density fluctuations at the short length scale focusing exclusively on spherical cavities. In this work, we use both first-principles and classical molecular dynamics simulations to demonstrate that density fluctuations in liquid water can deviate significantly from the canonical spherical shapes. We show that regions of empty space are frequently characterized by exotic, highly asymmetric shapes that can be quite delocalized over the hydrogen bond network. Interestingly, density fluctuations of these shapes are characterized by Gaussian statistics with larger fluctuations. An important consequence of this is that the work required to create non spherical cavities can be substantially smaller than that of spheres. This feature is also qualitatively captured by the Lum−Chandler−Weeks theory. The scaling behavior of the free energy as a function of the volume at short length scales is qualitatively different for the nonspherical entities. We also demonstrate that nonspherical density fluctuations are important for accommodating the hydrophobic amino acid alanine and are thus likely to have significant implications when it comes to solvating highly asymmetrical species such as alkanes, polymers, or biomolecules.

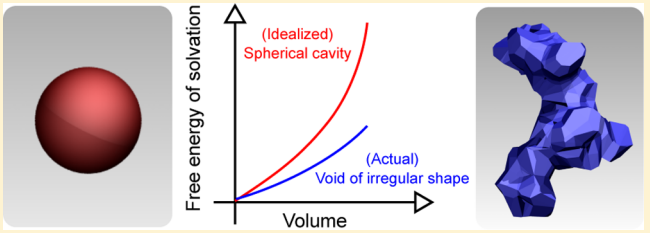

1. INTRODUCTION

Hydrophobic effects and hydrophobic interactions have significant implications in determining the structure, dynamics, aggregation, and subsequently the function of biomolecules in aqueous environments.[1−4] This is at the heart of important physical and chemical processes in biophysics such as protein folding and self assembly. One of the most fundamental and studied processes in this regard is the accommodation of hydrophobic solutes in water. From the point of view of thermodynamics, the first step of hydrophobic solvation involves determining the reversible work required to create an empty space or cavity in the hydrogen bond (HB) network. Understanding the microscopic and molecular ingredients of hydrophobic solvation has been the subject of numerous theoretical as well as experimental studies.[5−11]

Over the last few decades, there have been several theoretical and computational studies examining the molecular signatures of hydrophobicity.[6,12−16] An aspect of this problem that has consistently emerged is how solvent density fluctuations are altered in close vicinity to a hydrophobic surface.[17−20] In particular, the statistical mechanics of cavity (a connected region of empty space within the water network) formation and how this changes as a function of the size of the hydrophobic solute, has been shown to be a good measure of hydrophobicity. At the same time, the properties of density fluctuations provide a microscopic link between the small and large length scale hydrophobic effects where in the latter regime, the thermodynamics is driven by the surface energy of interface formation.[7,20]

For the most part, cavities in water are treated as highly idealized spherical objects. In this context, quantities such as the excess chemical potential for inserting a cavity in water, as used in the information theory for hydrophobic effects,[21] examine the number density fluctuations that occur within spherical regions. There have been recent studies examining the nature of

Received: November 7, 2016
Published: December 9, 2016

DOI: 10.1021/acs.jpca.6b11168
J. Phys. Chem. A 2017, 121, 370−380

density fluctuations (i.e., the geometrical and thermodynamical properties of regions of empty space forming within the water network) for nonspherical geometries such as cubes, cuboids, and cylinders.[22,23] The solvation thermodynamics of nonspherical shapes has also been explored with morphometric thermodynamics[24] and scaled-particle theory.[25] In another recent study, classical scaled particle theory was used to show that free energy for cavity formation depends on the geometry by an analysis comparing thermodynamics of sphere and spherocylindrical cavity formation in water.[26] However, these shapes are still idealized as they do not capture the actual shapes that emerge from microscopic inhomogeneities and molecular roughness that characterizes regions of free space in the HB network. Sulimov and co-workers examined the cavitation free energies of organic molecules consisting of different sizes and shapes with molecular dynamics simulations and found that for systems with an effective radii less than 7 Å, the computed free energies appeared to exhibit a linear dependence in the volume.[27] Recently, Pettitt and co-workers have examined the effects of geometry and chemistry on hydrophobic solvation of hydrocarbon molecules and found that hydrophobic theories built on assuming a simple linear dependence of the free energy of solvation on the surface area or volume were not consistent with their findings from simulations.[28] This evidence calls attention to the need of furthering our understanding of hydrophobic interactions to improve the current hydrophobic models.

In this work, we revisit the statistical properties of short length scale density fluctuations using molecular dynamics (MD) simulations of liquid water and show that the thermodynamics of the creation of realistic, nonspherical cavities in water is qualitatively different from that of spheres. In particular, we employ the Voronoi−Delaunay method[29] to characterize the regions of empty space within the water network. The resulting Voronoi−Delaunay voids (VDV) are characterized by a much richer diversity of morphologies when compared to the spherical cavities (SC) typically employed to investigate hydrophobicity at the molecular level. The VDV are highly nonspherical and rather than being localized in one region of the network, can often be spread across several solvation shells. The VDV we identify are subsequently used to examine the statistics of number density fluctuations as has been done previously for SC. We find that VDV are essentially *less hydrophobic* than SC because the work required to create them is substantially smaller compared to a SC of the same volume. Interestingly, the density fluctuations associated with VDV are well described by Gaussian fluctuations. Furthermore, the difference between the density fluctuations of SC and VDV is also qualitatively captured by the Lum−Chandler−Weeks (LCW) Gaussian field theory.[5] The microscopic fluctuations associated with hydrophobicity below the 1 nm length scale for the VDV are more nuanced than the picture built on the analysis of only SC leading to very different behavior in the transition from short-to-long length scale hydrophobic effects. The presence of asymmetric and exotic shapes in bulk water are a generic feature because we find that they are found not only in DFT-based *ab initio* water but also in two other water models, TIP4P-Ew[30] and, as illustrated in the Supporting Information, the MB-pol model.[31−33] We note that for processes that do not involve the dissociation of water, MB-pol is probably the most realistic model of molecular H_2O.

Understanding the density fluctuations of VDV has deep implications for water around and in the proximity of ions, rough molecular systems such as amino acids, proteins, and interfaces in general. Their branched and highly asymmetric character makes them good candidates for accommodating realistic small chemical systems. Here, we illustrate the possibility of these effects by examining the properties of the VDV that enclose the hydrophobic amino-acid alanine, in water. Similar to that of bulk water, the VDV distribution that engulfs alanine is highly asymmetric and requires less work to create than a SC of the same volume. The role of molecular roughness of both hydrophobic and polar organic molecules as manifested through the density fluctuations of VDV is an important future direction to explore in the area of hydrophobic effects.

2. COMPUTATIONAL DETAILS

2.1. Molecular Dynamics Simulations. Most of our analysis of both VDV and SC relies on the use of AIMD trajectories of periodic cubic liquid water boxes consisting of 128 water molecules. These simulations have recently been used to understand defect correlations in the HB network.[34] The reader is referred to the original paper for simulation details; however, we mention briefly that both the SC and VDV involved an analysis of four independent AIMD simulations with a total simulation length of 64 ps using the BLYP functional with Grimme's dispersion corrections. These simulations were thermostated at 300 K. It should be mentioned that obtaining large statistical samples of VDV is computationally expensive and the smaller AIMD systems make this process tractable. We were obviously concerned about whether the small system sizes and short simulation times would bias the density fluctuations and particularly the VDV statistics associated with p_0, which is the probability to find zero waters within the cavity as described in detail later. Classical MD simulations of a large (4096 molecules) model of bulk water have thus also been performed via the MD code LAMMPS.[35] Reconstructing the VDV for this big system is computationally prohibitive and hence VDV sampled from the AIMD simulation were used to examine p_0 obtained in the larger simulations. As explained in the manuscript, obtaining quantitative agreement with previous studies requires the use of classical MD simulations.

For the classical MD, water molecules have been modeled using the TIP4P-Ew[30] rigid water model. The density of water has been enforced to reproduce that of the AIMD simulations used in this work (0.0334 mol/Å^3), resulting in a cubic simulation box of length equal to 49.68 Å. The time step for the integration of the equations of motion and the coupling constant of the Nose−Hoover thermostat have been set to 2 and 1000 fs, respectively. The system was equilibrated at 270 K for 10 ns because the melting temperature for the TIP4P-Ew water model is $T_m \sim 244$ K. The 10^5 configurations used to accumulate statistics for both the SC and VDV (labeled SC_{T4} and VDV_{T4} for this system throughout the rest of the paper) have been extracted every 0.2 ps from a production run 20 ns long.

As alluded to in the Introduction, we also performed some analysis on water trajectories at 300 K using the MB-pol potential.[31−33] These simulations consist of 216 water molecules in a periodic cubic box of side length equal to 18.65 Å. Analysis of results obtained from MB-pol are shown in the Supporting Information (e.g., Figure S8).

2.2. Voronoi Voids. Our goal in this work was to determine the realistic shape and volume of regions of empty space within

DOI: 10.1021/acs.jpca.6b11168
J. Phys. Chem. A 2017, 121, 370−380

the water network. One popular approach used when dealing with bubble nucleation and cavitation in general[36,37] is to use grid-based methods where the simulation box is partitioned into three-dimensional regular cells usually of cubic shape. Volume elements that do not contain any atoms within them are subsequently connected to obtain the regions of empty space in the system. Despite the usage of these structured[38] grids due to their computational convenience, these probes are not related to the topological features of the atomic/molecular network, and as such, they usually cannot deal accurately with different atomic/molecular species for example, characterized by different van der Waals radii. Most importantly, taking into account highly nonspherical cavities by means of structured grids characterized by uniform cells size is often a challenging task as the volume elements have to be reduced down to a very small size, which in turn can lead to nonphysical pathways between different cavities.

For clarity, we remark that the analysis of the VDV we report here is distinct from evaluating the properties of Voronoi polyhedra of water which has been reported several times in the literature.[39,40] In fact, our analysis explicitly accounts for the atomistic structure of water molecules because the Voronoi S-network is a generalization of the Voronoi−Delaunay tessellation for multicomponent (or *polydisperse*) systems, namely, ensembles of atoms having different radii.

In this work, we adopt instead a flexible and robust approach based on the 3D Voronoi S-network proposed by Medvedev et al.[29,41] as implemented in the VNP program.[42] This methodology has been extensively employed to investigate cavities (or Voronoi−Delaunay voids, VDV) within a number of systems, including molecules in solutions[43] and complex interfaces.[44] We have also recently applied this particular framework to elucidate the emergence of nanocavities in semiconducting glasses[45] and to characterize the molecular mechanism of proton diffusion in water.[46] The 3D Voronoi S-network is a clever approach that builds upon the actual topology of the system, resulting in an unstructured three-dimensional grid capable of taking into account the complex, nonspherical shapes of empty regions in a HB network.

Here we review some of the essential concepts and refer the reader to the works by Medvedev et al. for details. In a polydisperse system, atomic volumes are delimited by the *Voronoi S surfaces* (VS surfaces). A VS surface is defined as the geometric locus of points equidistant from the surfaces of two atomic spheres instead of from their centers. VS surfaces are no longer planes as for Voronoi polyhedra but hyperboloids, and their intersection gives rise to curved edges (VS channels) and vertexes (VS vertexes). An interstitial sphere with radius R_I, tangent to neighbor atoms, is associated with each VS vertex whereas each VS channel is characterized by the radius R'_B of the largest test particle moving along that channel. The network of VS vertexes interlinked by VS channels can be used to distinguish interatomic voids and resolve connected cavities. In fact, a natural way of defining voids is through the value of the radius (R_P) of a test particle (probe) that can be put in the given void. Thus, voids are the parts of the interatomic space that are accessible for a given probe (i.e., $R_I \geq R_P$, R_I criterion). On the contrary, if a probe can move along an S-network bond (i.e., pass through a bottleneck), then both VS vertexes connected by that VS channel belong to the same cavity. Thus, if the extent of the bottleneck (represented by the radius R'_B of the largest test particle that would fit into it) is greater than a certain threshold R_B (which we refer to as *bottleneck radius* hereafter), the two regions are considered connected (i.e., $R'_B \geq R_B$, R_B criterion).

In our simulations, R_P has been set to 1.20 Å because the van der Waals radii of the hydrogen and oxygen atoms is 1.52 and 1.20 Å, respectively, whereas R_B has been set to 1.1 Å. The choice of R_B and R_P is important as they influence the number, the size, and even the morphology of the VDV. In a previous work[46] we have extensively investigated different choices of R_B and R_P leading to meaningful VDV characterized by bottlenecks of size comparable to that of a water molecule and quite often even larger (see, for example, Figure 1b). This is because the bottlenecks have to be larger than $R_B \cdot 2 = 2.2$ Å, an extent large enough to accommodate the hydrogen−hydrogen distance for a water and methane molecule, which is of the order of 1.65 and 1.75 Å, respectively. In addition, as in ref 46, we have checked that our results are consistent within a reasonable interval of values for both R_B and R_P. In particular, we have chosen R_B and R_P carefully to avoid very large volumes of empty spaces and very exotic VDV networks characterized by several bottlenecks, possibly percolating through the whole of the water network. As a result, the differences between VDV and SC reported in this work are likely to be even more pronounced in reality.

To compute the volume of voids, the space encompassed by the Voronoi S surfaces of the probe particles is calculated numerically through a local mesh, dense enough to minimize the residual below a threshold. Such voids are then eventually merged if they belong to the same cavity domain, according the R_B criterion, giving rise to an arbitrarily shaped cavity.

2.3. Cavity and Void Statistics. One of the central quantities discussed in this work is the probability $P(n)$ of observing n solvent centers (oxygens atoms in this case) within a SC or a VDV of a given volume. Such a probability has been obtained for a given SC or VDV by averaging n over 10^5 configurations coming from either ab initio or classical simulations. For each configuration, we have positioned the SC or VDV under analysis at the center of the simulation box and subsequently counting the number of oxygens that can be found within it. In this way, we have constructed the $P(n)$ reported in Figure 3. Although this process is straightforward for the SC and has been done in several previous studies,[21] handling the VDV requires special care. There is no ambiguity in the calculation of the VDV volume, as the geometrical definition of the VDV is unique once the system topology as well as the R_B and R_P parameters have been specified.

To probe whether a solvent center lies within the VDV or not, we have constructed for each VDV a corresponding 3D polyhedron, taking advantage of the alpha shape[47] construction available in MATLAB.[48] Such an object leads to a very fast computation of $P(n)$, as it allows us to establish quickly whether a point (in our case, an oxygen atom) lies in or out of the alpha shape, and thus within the VDV. The alpha shape construction for each VDV is not unique and depends on the alpha radius R_α, which in turn controls the level of detail of the alpha shape, or in other words how tightly the latter fits with respect to the original set of points (in our case, the vertices of the Delaunay simplexes involved in the VDV). Thus, the choice of R_α affects the volume as well as the surface area of the resulting alpha shapes, that is, of the 3D polygons by which we represent the VDV to compute $P(n)$. Hence, for each VDV we have determined R_α so that the volume of the corresponding alpha shape is consistent with the volume of the actual VDV within an accuracy of ±5 Å^3. We have also checked that

DOI: 10.1021/acs.jpca.6b11168
J. Phys. Chem. A 2017, 121, 370−380

different values of R_α lead to very similar results in terms of the predicted surface area, introducing an uncertainty of, at most, 5%, far too small to have any effect on the results reported in this work.

To extract the excess chemical potential $\Delta\mu$ for SC/VDV formation, we have fitted each $P(n)$ with a normal distribution $P_{\text{Gauss}}(n)$:

$$\Delta\mu = -k_B T \ln P_{\text{Gauss}}(n=0) \quad (1)$$

Here, k_B is the Boltzmann constant, T is the temperature, and $P_{\text{Gauss}}(n=0)$ is the value of $P(n)$ for $n = 0$. Consistent with previous theoretical and numerical studies, the $P(n)$ distributions for the SC are well described by Gaussian fluctuations. Perhaps more surprising, is that the larger asymmetric VDV are also characterized by Gaussian statistics.

3. VDV VS SC: STRUCTURAL PROPERTIES

To build our intuition on the results and discussions to follow, we begin by discussing the structural properties of the regions of empty space we are going to consider, described in terms of either spherical cavities (SC) or Voronoi−Delaunay voids (VDV). To this end, we illustrate in Figure 1 two different VDV

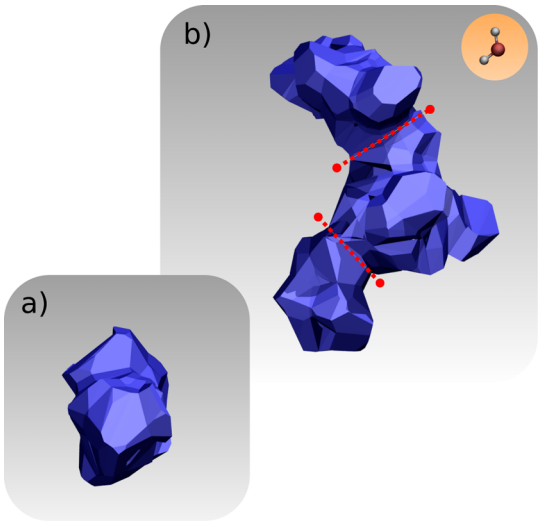

Figure 1. Typical shape of (a) small (∼50−100 Å^3) and (b) large (∼150−250 Å^3) VDV as found within a 128-mol model of ab initio water at room temperature. Though small VDV tend to be rather spherical and compact, larger ones often display rather complex, nonspherical shapes. Red dotted lines in panel b highlight the bottlenecks (see text) within the large VDV. The inset in panel b (top right) depicts a single water molecule on the same scale. The volume of the VDV is 88 and 249 Å^3 in panels a and b, respectively.

obtained from an ab initio molecular dynamics (AIMD) simulation of liquid water. Details of the MD simulations and the procedure employed to extract the VDV from the water network are discussed in section 2. Note that although the surface of the VDV has no analytic representation, it provides a convenient and robust numerical way to quantify the space enclosed by the VDV. Small (50−100 Å^3) VDV such as the one depicted in Figure 1a are typically rather spherical and compact. In contrast, large (150−250 Å^3) VDV such as the one shown in Figure 1b can be characterized by quite exotic shapes that deviate significantly from spherical symmetry. These morphologies emerge from the spontaneous fluctuations in the HB network, and in some cases they extend across several solvation shells. Though some of these large regions of empty space encompass just one convex polyhedron (Figure 1a), in many situations their branched shapes originate from the existence of bottlenecks (Figure 1b). It should be noted that in most cases these channels connecting two regions of empty space are wide enough to accommodate at least one water molecule. One can imagine how such branched VDV could provide the right ingredients to accommodate elongated shapes of molecules such as branched alkane chains and small peptides.

The VDV shown in Figure 1b already illustrates that there are likely to be regions of empty space that are much larger in volume and surface area than those one would predict looking exclusively at SC within the same water network. To see this more quantitatively, we show in Figure 2a the cumulative

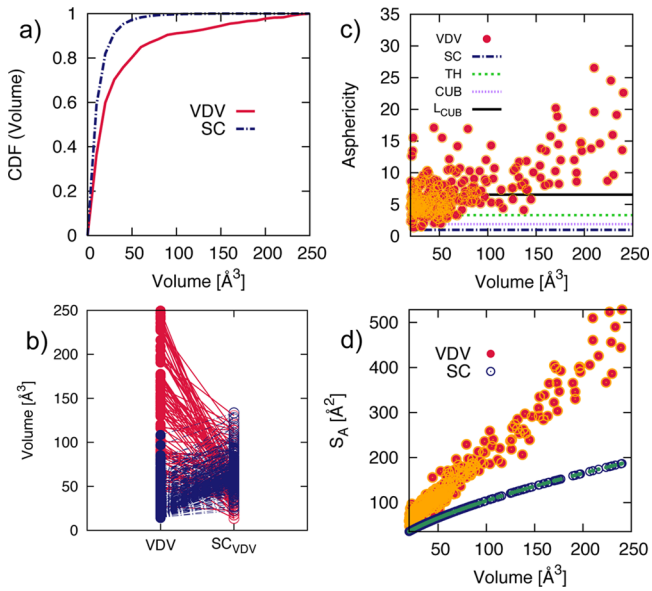

Figure 2. (a) Cumulative distribution function (CDF) of the volume of VDV and SC within the 128-mol model of ab initio water at room temperature. (b) Before−after plot for the VDV volume (left stack) and the volume of the largest SC one can build by sitting on the baricenter of the correspondent VDV (right stack). Points and segments for which VDV volume is smaller than SC_{VDV} volume are depicted in blue, whereas points and segments for which VDV volume is larger than SC_{VDV} volume are depicted in red. (c) Asphericity of VDV as a function of volume. Reference values for different regular shapes are also reported: SC, TH, CUB, and L_{CUB} refer to sphere, tetrahedron, cube, and asymmetrical cuboid. (d) Surface area S_A as a function of volume for SC and VDV.

distribution function (CDF) of the volume of SC and VDV within the water network that are observed from spontaneous thermal fluctuations at room temperature. Although the probability of finding SC of volume >100 Å^3 is basically zero, fat tails in the CDF for the VDV indicates the presence of sizable regions of empty space up to 200−250 Å^3. For the SC, a volume of 250 Å^3 corresponds to a SC with radius of about 4 Å. Needless to say, larger SC can possibly form in water but cannot be found within the relatively short times scale of our ab initio molecular dynamics (AIMD) simulation.

Probing the density fluctuations in water focusing exclusively on the SC does not capture the complexity of the underlying network originating from the molecular roughness and inhomogeneities in the 3D-structure of the hydrogen bond network. One way to see this is to look for SC that can form

DOI: 10.1021/acs.jpca.6b11168
J. Phys. Chem. A 2017, 121, 370−380

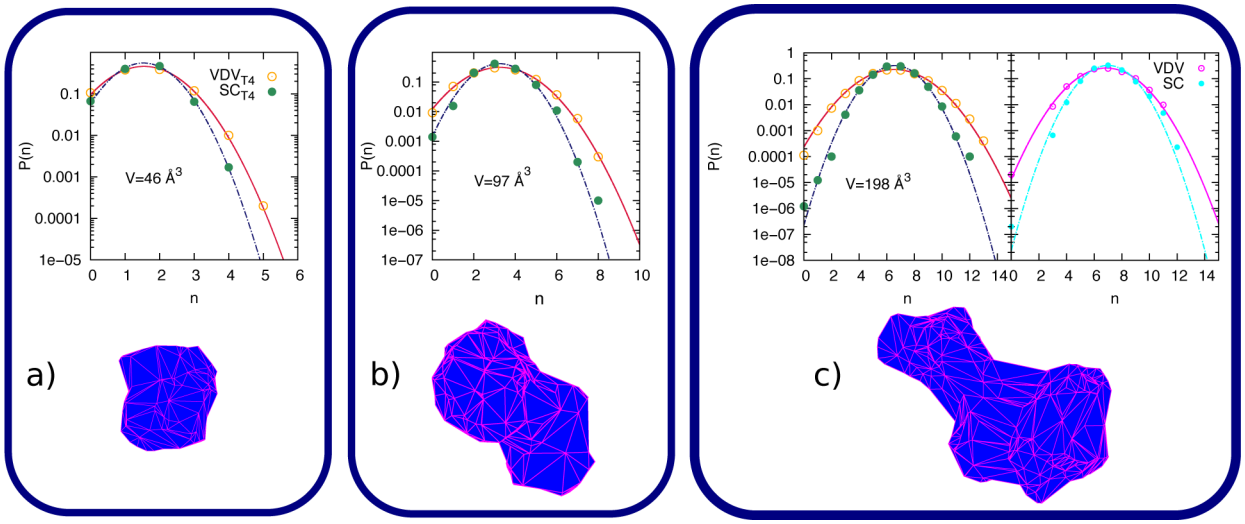

Figure 3. Probability $P(n)$ of observing n solvent centers (n oxygens) within VDV (VDV_{T4}) and a corresponding SC (SC_{T4}) of the same volume. Statistics has been accumulated over 10^5 configurations of a 4096-mol model of TIP4P/Ew water. Panels a–c report $P(n)$ for selected VDV of 46, 97, and 198 Å^3, respectively, together with insets showing the VDV shape as approximated via the alphaShape construction (see the Computational Details section). We also report in panel c (right side) the $P(n)$ obtained for the same VDV and SC (VDV and SC, respectively) but calculated using 10^5 configurations of a 128-mol model of BLYP water (section 2).

within nonspherical VDV. This is seen in Figure 2b where we report the volume of the VDV (left stack) against the volume of the largest SC (SC_{VDV}, right stack) that can be built by sitting on the center of mass of the corresponding VDV. First, we see that small (~50–100 Å^3) VDV are slightly smaller (dotted blue segments pointing upward from the VDV to SC_{VDV}) than the corresponding SC_{VDV}. This is because the surface of a SC exactly touches the closest atom with respect to its center of mass, whereas the Voronoi construction upon which the VDV are built implies that some space around the atoms is excluded according to the vdW radius of each atomic species. This feature holds for small VDV characterized by a fairly spherical shape. On the contrary, larger (~150–250 Å^3) VDV possess a much larger volume (solid red segments pointing downward) with respect to the corresponding SC_{VDV}. This is because large VDV are characterized by branched, nonspherical shapes including bottlenecks, which cannot be captured by SC.

Yet another probe into the complexity of the shape of the VDV is their asphericity, which can be quantified using the following expression:[49]

$$\eta = \frac{S_A^{\,3}}{36\pi V^2} \tag{2}$$

where S_A is the surface area of the VDV and V its volume. A scatter plot of η against the volume of the VDV is reported in Figure 2c together with the reference values for a regular sphere (SC), a regular tetrahedron (TH), a cube (CUB), and a very asymmetrical cuboid (L_{CUB}) characterized by an edge 10 times larger than the other two sides. One can clearly see that shapes of larger VDV in the HB network deviate significantly from idealized objects. In particular, a number of large VDV feature an asphericity value far greater than the most common regular polyhedra, including the elongated shape of L_{CUB}. This is due to the fact that the realistic regions of free space in the hydrogen bond network as probed by the VDV consist of highly corrugated objects characterized by a very large surface area as shown in Figure 2d. Details about the calculation of the surface area of the VDV are included in section 2.

In summary, our results up to this point show that the creation of the asymmetric and aspherical voids is a feature that is present in both DFT water and also the classical potential TIP4P/EW. As indicated earlier, we also repeated some of our analysis of the cavities using MB-pol, which indicates that the formation of the VDV is a generic property that is independent of the type of water model.

4. VDV VS SC: DENSITY FLUCTUATIONS AND THERMODYNAMICS OF SOLVATION

As alluded to earlier, one of the most important signatures and studied properties for understanding hydrophobicity are density fluctuations in bulk water[21] and near hydrophobic interfaces.[50] In this context, one often looks at the reversible work $\Delta\mu$ required to create a region of empty space within the water network. This free energy cost, often referred to as the *excess chemical potential* is related to the probability $P(n)$ of finding n solvent centers (in our case: oxygen atoms) within that particular empty region via the following relation:

$$\Delta\mu = -k_B T \ln P(n{=}0) \tag{3}$$

where k_B is the Boltzmann constant, T is the temperature of interest and $P(n{=}0)$ is the probability of finding zero solvent centers within the cavity. Further details can be found in the Computational Details section. Given the abundance of highly nonspherical VDV with different shapes in the HB network, we now move on to understanding the thermodynamics of their creation.

4.1. Gaussian Fluctuations for VDV. As described in more detail in the Computational Details section, constructing the VDV is quite computationally intensive and hence it is only feasible to extract these from the smaller AIMD simulations. Obvious concerns when using AIMD are the short simulation times (~10^2 ps) as well as the small system sizes (128 water molecules), for converging properties such as the $P(n)$. For this reason, we have computed the $P(n)$ by probing the density fluctuations from classical MD simulations as well. The classical simulations allow for the accumulation of statistics over ~10^4 ps for large (4096 water molecules) simulation boxes. Indeed,

DOI: 10.1021/acs.jpca.6b11168
J. Phys. Chem. A 2017, 121, 370–380

although AIMD and classical MD provide the same qualitative picture (as shown in Figure 3c), we will see that the classical simulations provide a description of the thermodynamics of solvation for SC in quantitative agreement with previous studies.[21] We thus report in Figure 3 the $P(n)$ obtained from the classical simulations using VDV that were extracted from the AIMD simulations. More details on this can be found in section 2.

The $P(n)$ shown in Figure 3 show that the density fluctuations associated with VDV are characterized by softer tails to both lower and higher n when compared to the $P(n)$ obtained for an SC of the same volume. This implies that $P(n=0)$ for the VDV is larger than what we observe for SC. In other words, eq 3 tells us that the free energy cost needed to create a VDV of a given size can be substantially smaller than that required to form a SC. It is worth stressing that this particular trend holds for the entire range of VDV volumes examined. In the Supporting Information (Figure S1 and Figure S2) we report the $P(n)$ for VDV and SC obtained from AIMD and classical simulations for some more SC and VDV.

Having assessed the properties of $P(n)$ for SC and VDV, we now turn our attention to the behavior of $\Delta\mu$ as a function of an effective length scale. The LCW theory predicts a characteristic length-scale behavior to the excess chemical potential for hydrophobic hydration. In particular, the theory predicts that at short length scales, the chemical potential is roughly proportional to the volume for spherical cavities. This feature is also captured by information theory and numerical simulations by Hummer and co-workers.[21] At longer length scales, $\Delta\mu$ is proportional instead to the surface area.[6]

To construct a similar analysis for the VDV, we need to provide a measure for its characteristic length. For the sake of simplicity, we define the length scale of the VDV as the radius required to generate a SC with the same volume. As we will see later, this *effective radius* underestimates how delocalized the VDV are over the network. This feature will be illustrated more explicitly later in the text. Figure 4a shows $\Delta\mu$ obtained from both the AIMD and classical simulations. Interestingly, the excess chemical potential characteristic of VDV is consistently lower than that of the SC with the same volume; the work required to create a VDV in this short-length scale regime is lower by about 10−15 kJ/mol. This feature is independent of the system size and simulation time because it is found in both AIMD and classical simulations. As mentioned earlier, our results from the classical simulations are in better agreement with an earlier study (see data of Hummer at al. shown in Figure 4a).

Our earlier results show that the density fluctuations associated with SC or VDV are well characterized by Gaussian statistics. Within this assumption, one can write[51] an analytic expression for $\Delta\mu$ as

$$\Delta\mu \sim k_B T \cdot \frac{\rho_w^{\,2} V^2}{2\chi_V} + k_B T \cdot \frac{\ln(2\pi\chi_V)}{2} \tag{4}$$

where ρ_w, V, and χ_V are the water density, the volume of the VDV/SC and the variance of $P(n)$ for that particular VDV/SC respectively. The second term of eq 4 depends logarithmically on χ_V, so that it is often neglected. In the Supporting Information (Figure S4a) we show that indeed the inclusion of such a term does not change the qualitative trend that sees VDV having a substantially lower $\Delta\mu$ if compared to SC of the same volume. Gaussian statistics of the $P(n)$ as observed for

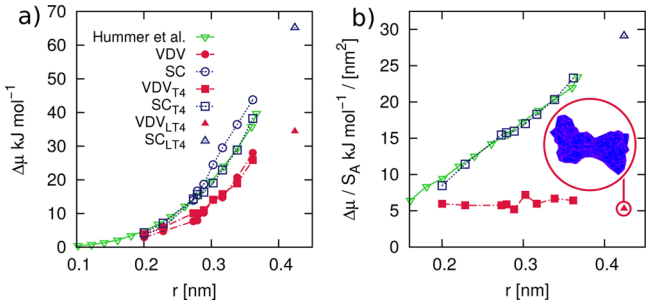

Figure 4. (a) Excess chemical potential $\Delta\mu$ as a function the *radius r* of SC and VDV. For VDV, r is defined as the radius of a sphere with exactly the same volume as the VDV. Note, however, that $\Delta\mu$ has been obtained from the $P(n)$ calculated using actual VDV with shapes like those depicted in Figure 1 and Figure 3. We also show $\Delta\mu$ for the same SC and VDV evaluated within 10^5 configurations of a 16384-mol model of TIP4P/Ew water (SC$_{T4}$ and VDV$_{T4}$, see text). The excess chemical potential for a large VDV found within the TIP4P/Ew model and its corresponding SC are labeled as VDV$_{LT4}$ and SC$_{LT4}$ (see text for details). Data for SC reported in the work of Hummer et al.[21] are also reported. (b) Excess chemical potential divided by surface area as a function of volume for SC and VDV. Data for the same SC and VDV evaluated within 10^5 configurations of a 4096 water molecule model of TIP4P/Ew water (SC$_{T4}$ and VDV$_{T4}$, see text) are also reported, together with the result obtained for a large VDV found within the TIP4P/Ew model and its corresponding SC, labeled as VDV$_{LT4}$ and SC$_{LT4}$. The subscript LXT4 corresponds to the largest VDV that was found by performing the Voronoi analysis on the TIP4P/Ew simulations.

both the SC and VDV rationalizes the trends observed in $\Delta\mu$ shown in Figure 4. For SC, $\chi_V \sim V$,[7] so that $\Delta\mu \sim k_B T \cdot \rho_w^{\,2} V$. However, for the VDV examined here $\chi_V \sim V^\alpha$ with $\alpha = 1.07 \pm 0.01$, which in turn leads to a lower $\Delta\mu$ for VDV compared to that of the corresponding SC. Although the change in the value of alpha is small, we will see later that the difference in the behavior of $\Delta\mu/S_A$ for SC and VDV can be rationalized by the subtle differences in the exponents such as α within the Gaussian theory. See the Supporting Information for more details on how the χ_V scales with the volume for SC and VDV (Figure S4b).

4.2. VDV vs SC: Behavior of $\Delta\mu/S_A$. The preceding analysis shows that the thermodynamics of VDV formation is quite different from that of SC. From an intuitive point of view, one way to rationalize this behavior is that the larger amounts of free space associated with VDV originate from the inherent 3D-architecture of the HB network, which naturally creates regions of depleted density in water, as we shall see later. This creates small vapor-like tunnels or bottlenecks, as seen in Figure 1b, which result from connected smaller regions of depleted density. On the contrary, the construction of large spheres requires a much larger localized depletion of density. To appreciate the effect of the differences between VDV and SC on the length-scale dependence to the hydrophobic effect, we recall that the surface area of the VDV exhibits a much stronger volume dependence than that showed by the SC, as reported in Figure 2d. For instance, VDV of about 200 Å^3 can have a surface area twice as large as the SC of the same volume. This feature has critical consequences with respect to the excess chemical potential per unit area, $\Delta\mu/S_A$, reported for both VDV and SC in Figure 4b. In the case of SC, the $\Delta\mu/S_A$ that has to be paid to create larger regions of empty space in the water network increases linearly with the radius of the SC consistent with previous observations from information theory and

DOI: 10.1021/acs.jpca.6b11168
J. Phys. Chem. A 2017, 121, 370−380

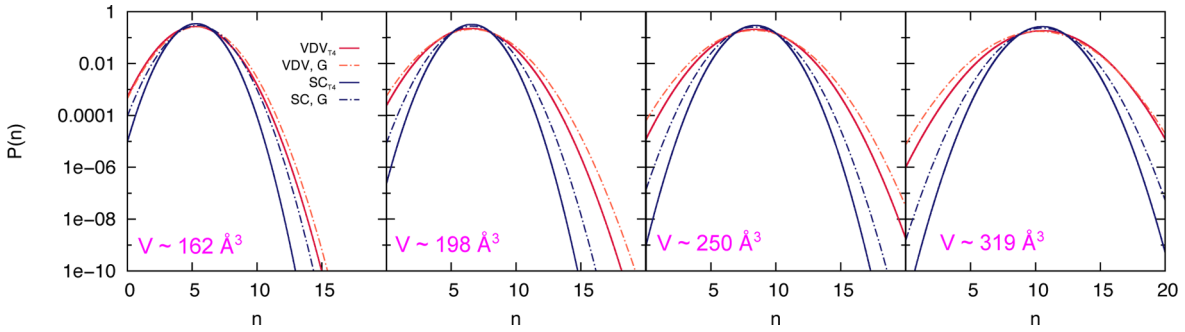

Figure 5. Probability $P(n)$ of observing n solvent centers (n oxygens) within VDV (VDV_{T4}) and a corresponding SC (SC_{T4}) of the same volume. Statistics has been accumulated over 10^5 configurations of a 4096-mol model of TIP4P/Ew water. The results obtained within the Gaussian approximation (see text) for VDV (VDV,G) and SC (SC,G) are also reported as dotted lines.

molecular simulations.[21] In contrast, despite having a much larger surface area, creating large VDV costs less energy and $\Delta\mu/S_A$ for the VDV is basically constant on the length-scale quantified by their effective-radii.

Without employing any sophisticated sampling methods like those developed by Patel and co-workers[22,23] to probe larger length scales of realistic VDV, we cannot conclusively say how $\Delta\mu/S_A$ approaches the macroscopic surface tension. However, the value of $\Delta\mu/S_A$ we obtain for VDV is ~6 kJ mol^{-1}/nm^{-2}, which is roughly 15% of the macroscopic surface tension of the air−vapor interface and 26% of the *effective* surface tension reported for idealized shapes by Patel and co-workers.[22] It is clear from the preceding analysis that the short-length scale behavior of hydrophobic effects for VDV is quite different from that of SC and that the details of the shape and geometry of hydrophobic cavities will play an important role in how abruptly the short-to-long hydrophobic behavior occurs.

4.3. VDV vs SC: LCW Theory. Molecular simulations by Hummer and co-workers have demonstrated that small length scale density fluctuations in liquid water are remarkably Gaussian.[21] Indeed, the results reported in Figure 3 indicate that the $P(n)$ for both SC and VDV can be well described by Gaussian fluctuations. According to the LCW framework, density fluctuations at long and short wavelengths, corresponding to the emergence of large and small cavities within the water network respectively, are treated separately: though a purely Gaussian description is sufficient to deal with small (i.e., subnanometer scale) cavities, the thermodynamics of larger regions of empty space is dominated by the macroscopic surface tension. As such, the large distortions of the density field associated with the occurrence of such large cavities are typically resolved by coarse-graining the water network on a lattice.[23] This approach requires only the experimentally determined bulk pair correlation function and macroscopic surface tension as inputs and is capable of dealing with density fluctuations involving very different length scales.[52]

To understand whether LCW theory is capable of describing the highly nonspherical density fluctuations resulting in the formation of the VDV, we compare in Figure 5 the $P(n)$ for selected SC and VDV we have obtained from the Gaussian fits of the atomistic simulations (SC/VDV_{T4}, obtained in the same fashion to those reported in Figure 3), with those calculated from LCW theory using only the Gaussian contribution (labeled SC/VDV,G; see refs 23 and 52 for further details). Fatter tails in the $P(n)$ for VDV,G with respect to SC,G can be observed for all the SC/VDV considered, in agreement with the SC/VDV_{T4} data. Thus, LCW theory confirms that the free energy cost needed to form a VDV of a given volume can be significantly lower than that required to create a SC of the same volume. Thus, the difference in thermodynamics observed for SC and VDV is essentially encoded by the fluctuations underlying the pair correlation function of liquid water.

We note that although LCW theory predicts fatter tails of the VDV distributions compared to those of SC, the agreement with the numerical simulations is not quantitative; in fact, the errors appear to be slightly larger for the SC than the VDV. The origin of these differences is associated with errors originating from numerical integration and discretization.[23,52] In earlier studies, it was also shown that the long-wavelength lattice fluctuations were important for spheres of radii larger than 0.5 nm. To assess whether lattice fluctuations improve the characterization of the $P(n)$ for the larger more delocalized VDV, distributions were constructed including the lattice contribution. Although there is some indication that doing so improves the $P(n)$ for the VDV, lattice fluctuations do introduce large errors due to the small length scales of the SC/VDV considered in this work and hence we focus on only qualitative trends (see the Supporting Information for more details).

5. HB NETWORK IN PROXIMITY OF VDV

Our analysis alluded to the delocalized nature of the VDV across the HB network. It is interesting to examine whether these features result in any significant disruption of the HB network. One way to probe this is to examine certain topological properties in water such as the deviation of the water molecules enveloping a VDV from local tetrahedrality. To quantify this, we examined both the in-degree (the number of HB being accepted by a water molecule) and the out-degree (the number of HB being donated) of water molecules that are within 2 Å of the vertices of the Voronoi-polyhedra enclosing the VDV. A similar analysis was recently performed on bulk water looking at defect correlations in the network.[34] In this study, it was found that independent of the choice of the water model, most water molecules in bulk water accepted and donated two HB and that thermal fluctuations result in defects that cluster together. For the water molecules enveloping the VDV, the notion of their origin emerging from natural fluctuations is reinforced. In fact, the distributions of the in and out degrees show that most of these waters are tetrahedral; there is no signature of an increase in the number of defect water molecules such as over- or undercoordinated water molecules compared to the case for bulk water (Figure S5 in the Supporting Information).

DOI: 10.1021/acs.jpca.6b11168
J. Phys. Chem. A 2017, 121, 370−380

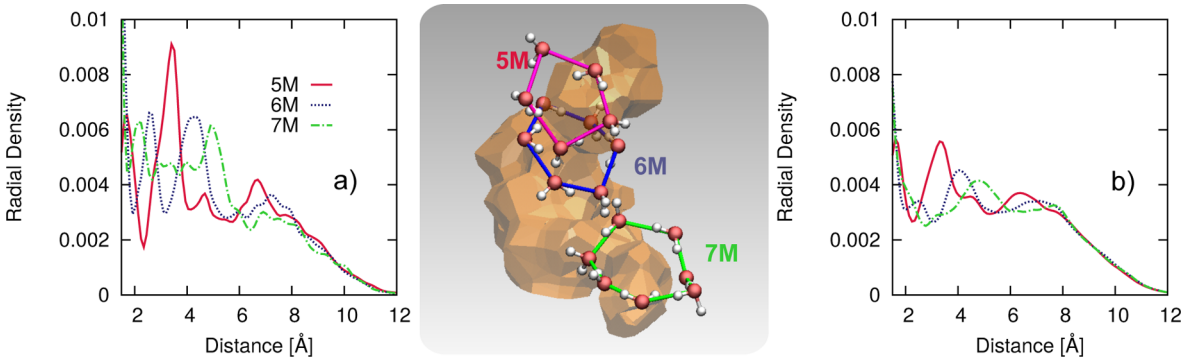

Figure 6. Radial density distribution between the center of mass of five-, six-, and seven-membered (a) closed rings enveloping the VDV (depicted in the central inset) and (b) closed rings in the whole of the water network. The solid red, dotted blue, and dashed green curves correspond to the 5−5, 6−6, and 7-M radial distributions.

The presence of the large VDV in the network can also be probed through the lens of other topological parameters. In liquid water, it is well-known that local tetrahedrality results in the presence of closed rings having specific directional correlations leading subsequently to medium-range water wires.[53] The extended VDV can be viewed as resulting from the specific correlations of the arrangement of rings with different sizes in the 3D-network. To examine this in more detail, we studied the radial density distributions between the center of mass of rings enveloping the VDV. As we did earlier for the defect distributions, rings were identified for water molecules within 2 Å of the vertices of the Voronoi-polyhedra. Figure 6a shows the radial densities obtained between all five-, six-, and seven-membered rings enveloping large VDV, indicating correlations extending up to ∼8 Å. The 3D stacking of the closed rings and their corresponding fluctuations are not unique or exclusive to the immediate environment around a VDV. To see this more clearly, Figure 6b illustrates the radial densities between the same sized rings, now averaged over all the rings in the water network. The distributions are indeed quite similar and reinforce the notion that the VDV are formed by the inherent correlations of the 3D HB network. The 3D-stacking of closed closed rings in the network essentially provides an intuitive way to understand how the VDV form.

These findings suggest that the creation of even significantly large (∼250 Å^3) VDV does not require a sizable disruption of the HB network. It would be interesting in future studies to examine how the formation of larger idealized shapes such as spheres or cuboids alter properties such as the distribution of rings as well as local topological defects associated with the coordination of water molecules.

6. VDV VS SC: SOLVATION OF HYDROPHOBIC SOLUTES

Understanding the role of density fluctuations in the creation of VDV around hydrophobic solutes and proteins is beyond the scope of the current study. However, as hydrophobic interactions are of paramount importance in important physical and chemical processes in biophysics such as protein folding and the aggregation of biomolecules, we wanted to assess the role of nonspherical VDV in solvating a realistic hydrophobic molecule. In particular, the comparison of $\Delta\mu$ for VDV vs SC naturally occurring in bulk water (Section 4.1 and, e.g., Figure 4), shows that the excluded volume contribution to the solvation energy is very sensitive to the shape. Here we focused on the hydrophobic amino-acid alanine; using AIMD simulations of a single alanine residue in water, we determined the volume and surface area of the VDV in the water network identified after the residue is removed. The VDV identified was then used to examine whether it would naturally emerge from fluctuations in bulk water, as we did before, as well as to understand how the thermodynamics of their formation would compare with an SC of the same volume.

The VDV volume distribution peaks at about 100 Å^3 with a rather broad distribution ranging between 60 and 200 Å^3 (Supporting Information Figure S6a). Similar to those in bulk water, the VDV enveloping alanine are highly asymmetric with much more exotic shapes than that inferred from SC. On the basis of using the volume, surface area, and asphericity measures (reported in the Supporting Information, see Figure S6b and Figure S6c), these VDV fall within the range of those naturally occurring from thermal fluctuations in bulk water. It is indeed interesting to see that the natural fluctuations of the HB network in bulk water, such as the one depicted in the inset of Figure 7, create the appropriate excluded volume to accommodate the hydrophobic amino acid alanine.

Similar to what was shown for bulk water, the excess chemical potential for the VDV is smaller than the SC by about 5−10 kJ/mol, as illustrated in Figure 7a. Note that $\Delta\mu$ has been obtained using the same set of 10^5 configurations of a 4096-mol model of TIP4P/Ew water employed for the $P(n)$ reported in Figure 3 (VDV/SC$_{T4}$). Figure 7b shows $\Delta\mu/S_A$ for the VDV and SC; once again, the scaling behavior is very different as observed earlier for the cavities in bulk water. For the VDV, $\Delta\mu/S_A$ is essentially flat over the volume range explored and takes on a numerical value very close to that observed earlier in bulk water, which is a small fraction of the macroscopic surface tension of the air−water interface. Thus, intrinsic molecular roughness of the realistic shapes that enclose the alanine residue increases the importance of surface area in hydrophobic solvation at short length scales. Due to the small simulation box sizes used to analyze these effects, we cannot make quantitative statements about the VDV in the water network outside of the amino acid. However, an examination of the fluctuations around alanine shows that there are rather large asymmetric VDV regions extending from the hydrophobic moiety, as seen in the inset of Figure 7. This evidence is far for being trivial: the fact that even a small hydrophobic molecule such as the alanine residue considered here is capable of originating regions of empty space extending well beyond the neighboring water molecules suggests that larger objects such as proteins can

DOI: 10.1021/acs.jpca.6b11168
J. Phys. Chem. A 2017, 121, 370−380

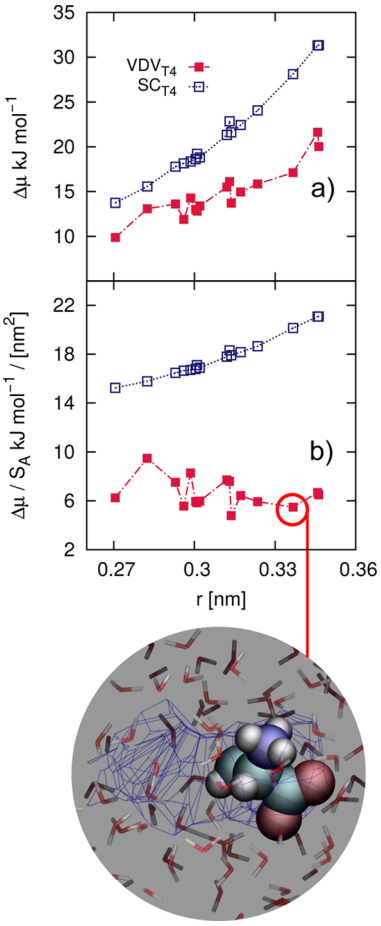

Figure 7. Excess chemical potential for a randomly selected subset of the VDV (and the corresponding SC of the same volume) created by removing the alanine molecule from the water network. Results are averaged over $\sim 10^3$ configurations. The inset depicts a frequent situation where the presence of the alanine molecule produces a VDV that is substantially larger than the size of the molecule itself.

substantially alter the topology and the thermodynamics of density fluctuations in liquid water.

7. DISCUSSION AND CONCLUSIONS

One of the most important cornerstones of hydrophobic effects is its sensitivity to the underlying length scale of the associated hydrophobic solute. On the one hand, at short length scales, a combination of both analytic theories and numerical simulations have shown that Gaussian statistics accurately characterize density fluctuations. On the other hand, at larger length scales, the thermodynamics of hydrophobic solvation is driven by interface formation. The vast majority of theoretical studies in this area focus on the formation of idealized spherically SC. The work ($\Delta\mu$) required to create a SC grows as the volume and hence $\Delta\mu/S_A$ grows as the radius of a sphere (see Figure 2 of ref 7).

In this work, we revisited the picture that has been constructed for the behavior of short length scale density fluctuations built upon focusing exclusively on SC. The shape of hydrophobic solutes has been shown to be important, for example, in anion binding in the context of understanding Hofmeister chaotropes[54] as well as in the solvation of hydrocarbons[28] and other organic molecules.[27] A key message of this work is that the molecular shape of voids in water has important implications on the physics of hydrophobic solvation. In particular, we extract an exotic mixture of VDV that are formed by natural fluctuations of the HB network using a Voronoi analysis. The regions of excluded volume in the water network are highly asymmetric and can extend over rather large regions of the HB network. The molecular origins of these features are shown to come from inherent features of the 3D network of water such as the stacking of closed rings across several hydration shells. Density fluctuations of the VDV are well characterized by Gaussian statistics. An interesting consequence of this is that the variance associated with these fluctuations is larger for VDV compared to SC of the same volume. Thus, despite having a much larger surface area than spheres of the same volume, the work required to create VDV is much smaller.

The scaling behavior of $\Delta\mu/S_A$ is qualitatively different for the VDV compared to SC. On the length scales currently probed from spontaneous thermal fluctuations, $\Delta\mu/S_A$ is effectively constant. The origin of this behavior appears to be well explained by the Gaussian theory: the larger width of the $P(n)$ for VDV results in $\Delta\mu \sim k_BT\cdot\rho_w{}^2V^\beta$ with $\beta < 1$. At the same time, the surface area of the VDV also has a nontrivial volume dependence. In particular for SC, the surface area scales exactly as $V^{2/3}$, whereas for the VDV, our numerical simulations suggest that the surface area grows as $V^{0.82\pm0.01}$ (see the Supporting Information for more details, Figure S4c). Subsequently, $\Delta\mu/S_A$ grows as $V^{1/3}$ and $V^{0.10\pm0.014}$ for SC and VDV, respectively (Figure S5a and b). As indicated earlier, the exponents we extract here provide a qualitative way to rationalize the difference in the thermodynamics of scaling behavior of SC vs VDV within using the Gaussian theory. The physics of short length-scale density fluctuations in water are clearly different for SC and VDV. Given that the VDV we examine represent those that are most easily formed, our results probe the lowest boundary in the space of $\Delta\mu/S_A$ and volume or effective radius. It is likely that there will exist other types of VDV covering the thermodynamic region between SC and the VDV. Our results also pose interesting challenges for theory to predict the solvation of hydrophobic solutes that go beyond exclusively concave or convex shapes. In this work, we focused on density fluctuations at ambient conditions only; it is clear that exploring the properties of VDV across the phase diagram of water would be an important and interesting extension of this study in the future.

Our focus in this work is on the characterization of static properties of the VDV. An obvious question of interest is on the lifetime of the VDV. Qualitatively, on the basis of visual inspection, small VDVs of volume $\sim$50−80 Å^3 survive for less than a picosecond. However, larger VDV of volume greater than 150 Å^3 can survive for time scales of up to 5 ps. During these time windows, the shape and volume of the VDV will obviously change. It will be interesting in the future to come up with more quantitative measures of the lifetime of VDV of different size and shape and perhaps more interestingly, develop experimental probes of SC and VDV in water. Besides its obvious interest in fundamental chemical physics of hydrophobic effects in bulk water, understanding the properties of VDV has deep implications on the solvation of solutes in general. For instance, we have shown in a previous work[46] that proton transfer in liquid water can be promoted by the occurrence of particular VDV, capable of facilitating an umbrella-like flip of the hydronium. In turn, this peculiar inversion mode of the charged species alters the free energy

DOI: 10.1021/acs.jpca.6b11168
J. Phys. Chem. A 2017, 121, 370−380

barrier for proton transfer. Though it is clear that providing a detailed understanding of the role of VDV in the solvation of realistic amino acids as well as in processes such as protein folding and ion solvation is beyond the scope of this work, we attempted to shed some light on this for the hydrophobic amino acid alanine. Interestingly, the natural fluctuations of the HB network create VDV that would accommodate the excluded volume region needed for alanine. It will be interesting to examine these features for other amino acids as well as molecules with different types of branching and roughness. Furthermore, it will also be interesting in the future to revisit the analysis of density fluctuations around proteins and near hydrophobic and hydrophilic interfaces that have typically been probed using idealized spheres.[50]

■ ASSOCIATED CONTENT

Supporting Information

The Supporting Information is available free of charge on the ACS Publications website at DOI: 10.1021/acs.jpca.6b11168.

This includes: the probability $P(n)$ of finding n solvent centers within the spherical cavities (SC) and Voronoi–Delaunay voids (VDV); lattice model results with respect to SC and the VDV; scaling exponent of the excess free energy of the solvation as a function of the volume and surface area; structural properties of the water network in the neighborhood of the VDV; statistics of VDV as obtained for the solvation of alanine in water; VDV and SC in MB-pol water (PDF)

■ AUTHOR INFORMATION

Corresponding Authors

*G. C. Sosso. E-mail: g.sosso@ucl.ac.uk.

*A. Hassanali. E-mail: ahassana@ictp.it.

ORCID

Gabriele Cesare Sosso: 0000-0002-6156-7399

Notes

The authors declare no competing financial interest.

■ ACKNOWLEDGMENTS

The authors are grateful to M. Ceriotti for providing the MB-pol molecular dynamics trajectory discussed in the SM. G.C.S. thanks P. Pedevilla, J. Chen, and G. Brandenburg for commenting on the original manuscript. G.C.S. also acknowledges the use of the UCL GRACE High Performance Computing Facility and of the ARCHER UK National Supercomputing Service (http://www.archer.ac.uk) via the Materials Chemistry Consortium through the EPSRC grant number EP/L000202.

■ REFERENCES

(1) Blokzijl, W.; Engberts, J. B. F. N. Hydrophobic Effects. Opinions and Facts. *Angew. Chem., Int. Ed. Engl.* **1993**, *32*, 1545–1579.

(2) Pratt, L. R. Theory of Hydrophobic Effects. *Annu. Rev. Phys. Chem.* **1985**, *36*, 433–449.

(3) Pratt, L. R.; Pohorille, A. Hydrophobic Effects and Modeling of Biophysical Aqueous Solution Interfaces. *Chem. Rev.* **2002**, *102*, 2671–2692.

(4) Ben-Amotz, D. Hydrophobic Ambivalence: Teetering on the Edge of Randomness. *J. Phys. Chem. Lett.* **2015**, *6*, 1696–1701.

(5) Lum, K.; Chandler, D.; Weeks, J. D. Hydrophobicity at Small and Large Length Scales. *J. Phys. Chem. B* **1999**, *103*, 4570–4577.

(6) Huang, D. M.; Chandler, D. Temperature and Length Scale Dependence of Hydrophobic Effects and their Possible Implications for Protein Folding. *Proc. Natl. Acad. Sci. U. S. A.* **2000**, *97*, 8324–8327.

(7) Chandler, D. Interfaces and the Driving Force of Hydrophobic Assembly. *Nature* **2005**, *437*, 640–647.

(8) Garde, S.; Patel, A. J. Unraveling the Hydrophobic Effect, one Molecule at a Time. *Proc. Natl. Acad. Sci. U. S. A.* **2011**, *108*, 16491–16492.

(9) Li, I. T. S.; Walker, G. C. Signature of Hydrophobic Hydration in a Single Polymer. *Proc. Natl. Acad. Sci. U. S. A.* **2011**, *108*, 16527–16532.

(10) Wang, J.; Bratko, D.; Luzar, A. Probing Surface Tension Additivity on Chemically Heterogeneous Surfaces by a Molecular Approach. *Proc. Natl. Acad. Sci. U. S. A.* **2011**, *108*, 6374–6379.

(11) Mittal, J.; Hummer, G. Static and Dynamic Correlations in Water at Hydrophobic Interfaces. *Proc. Natl. Acad. Sci. U. S. A.* **2008**, *105*, 20130–20135.

(12) Pratt, L. R.; Chandler, D. Theory of the Hydrophobic Effect. *J. Chem. Phys.* **1977**, *67*, 3683–3704.

(13) Hummer, G.; Garde, S.; Garcia, A. E.; Paulaitis, M. E.; Pratt, L. R. Hydrophobic Effects on a Molecular Scale. *J. Phys. Chem. B* **1998**, *102*, 10469–10482.

(14) Ghosh, T.; Garcia, A. E.; Garde, S. Molecular Dynamics Simulations of Pressure Effects on Hydrophobic Interactions. *J. Am. Chem. Soc.* **2001**, *123*, 10997–11003.

(15) Rajamani, S.; Truskett, T. M.; Garde, S. Hydrophobic Hydration from Small to Large Lengthscales: Understanding and Manipulating the Crossover. *Proc. Natl. Acad. Sci. U. S. A.* **2005**, *102*, 9475–9480.

(16) Ashbaugh, H. S.; Pratt, L. R. Colloquium: Scaled Particle Theory and the Length Scales of Hydrophobicity. *Rev. Mod. Phys.* **2006**, *78*, 159–178.

(17) Sarupria, S.; Garde, S. Quantifying Water Density Fluctuations and Compressibility of Hydration Shells of Hydrophobic Solutes and Proteins. *Phys. Rev. Lett.* **2009**, *103*, 037803.

(18) Patel, A. J.; Varilly, P.; Chandler, D. Fluctuations of Water near Extended Hydrophobic and Hydrophilic Surfaces. *J. Phys. Chem. B* **2010**, *114*, 1632–1637.

(19) Jamadagni, S. N.; Godawat, R.; Garde, S. Hydrophobicity of Proteins and Interfaces: Insights from Density Fluctuations. *Annu. Rev. Chem. Biomol. Eng.* **2011**, *2*, 147–171.

(20) Patel, A. J.; Varilly, P.; Jamadagni, S. N.; Acharya, H.; Garde, S.; Chandler, D. Extended Surfaces Modulate Hydrophobic Interactions of Neighboring Solutes. *Proc. Natl. Acad. Sci. U. S. A.* **2011**, *108*, 17678–17683.

(21) Hummer, G.; Garde, S.; Garcia, A. E.; Pohorille, A.; Pratt, L. R. An Information Theory Model of Hydrophobic Interactions. *Proc. Natl. Acad. Sci. U. S. A.* **1996**, *93*, 8951–8955.

(22) Patel, A.; Varilly, P.; Chandler, D.; Garde, S. Quantifying Density Fluctuations in Volumes of All Shapes and Sizes Using Indirect Umbrella Sampling. *J. Stat. Phys.* **2011**, *145*, 265–275.

(23) Vaikuntanathan, S.; Geissler, P. L. Putting Water on a Lattice: The Importance of Long Wavelength Density Fluctuations in Theories of Hydrophobic and Interfacial Phenomena. *Phys. Rev. Lett.* **2014**, *112*, 020603.

(24) Jin, Z.; Kim, J.; Wu, J. Shape Effect on Nanoparticle Solvation: A Comparison of Morphometric Thermodynamics and Microscopic Theories. *Langmuir* **2012**, *28*, 6997–7006.

(25) Ashbaugh, H. S. Scaled-particle Theory Analysis of Cylindrical Cavities in Solution. *Phys. Rev. E* **2015**, *91*, 042315.

(26) Graziano, G. The Gibbs energy cost of cavity creation depends on geometry. *J. Mol. Liq.* **2015**, *211*, 1047–1051.

(27) Grigoriev, F. V.; Basilevsky, M. V.; Gabin, S. N.; Romanov, A. N.; Sulimov, V. B. Cavitation Free Energy for Organic Molecules Having Various Sizes and Shapes. *J. Phys. Chem. B* **2007**, *111*, 13748–13755.

(28) Harris, R. C.; Pettitt, B. M. Effects of Geometry and Chemistry on Hydrophobic Solvation. *Proc. Natl. Acad. Sci. U. S. A.* **2014**, *111*, 14681–14686.

(29) Alinchenko, M. G.; Anikeenko, A. V.; Medvedev, N. N.; Voloshin, V. P.; Mezei, M.; Jedlovszky, P. Morphology of Voids in

Molecular Systems. A Voronoi-Delaunay Analysis of a Simulated DMPC Membrane. *J. Phys. Chem. B* **2004**, *108*, 19056−19067.
(30) Horn, H. W.; Swope, W. C.; Pitera, J. W.; Madura, J. D.; Dick, T. J.; Hura, G. L.; Head-Gordon, T. Development of an Improved Four-Site Water Model for Biomolecular Simulations: TIP4P-Ew. *J. Chem. Phys.* **2004**, *120*, 9665.
(31) Babin, V.; Leforestier, C.; Paesani, F. Development of a "First Principles" Water Potential with Flexible Monomers: Dimer Potential Energy Surface, VRT Spectrum, and Second Virial Coefficient. *J. Chem. Theory Comput.* **2013**, *9*, 5395−5403.
(32) Babin, V.; Medders, G. R.; Paesani, F. Development of a "First Principles" Water Potential with Flexible Monomers. II: Trimer Potential Energy Surface, Third Virial Coefficient, and Small Clusters. *J. Chem. Theory Comput.* **2014**, *10*, 1599−1607.
(33) Medders, G. R.; Babin, V.; Paesani, F. Development of a "First-Principles" Water Potential with Flexible Monomers. III. Liquid Phase Properties. *J. Chem. Theory Comput.* **2014**, *10*, 2906−2910.
(34) Gasparotto, P.; Hassanali, A. A.; Ceriotti, M. Probing Defects and Correlations in the Hydrogen-Bond Network of ab Initio Water. *J. Chem. Theory Comput.* **2016**, *12*, 1953−1964.
(35) Plimpton, S. Fast Parallel Algorithms for Short-Range Molecular Dynamics. *J. Comput. Phys.* **1995**, *117*, 1−19.
(36) Wang, Z.-J.; Valeriani, C.; Frenkel, D. Homogeneous Bubble Nucleation Driven by Local Hot Spots: A Molecular Dynamics Study. *J. Phys. Chem. B* **2009**, *113*, 3776−3784.
(37) González, M. A.; Menzl, G.; Aragones, J. L.; Geiger, P.; Caupin, F.; Abascal, J. L. F.; Dellago, C.; Valeriani, C. Detecting Vapour Bubbles in Simulations of Metastable Water. *J. Chem. Phys.* **2014**, *141*, 18C511.
(38) Structured grids differ from unstructured ones mainly in that the former are regularly connected, whereas the latter are charecterized by an irregular connectivity, that is, the way by which the vertices of the grid specify the volume elements. See, e.g., ref 55.
(39) Jedlovszky, P. The Local Structure of Various Hydrogen Bonded Liquids: Voronoi Polyhedra Analysis of Water, Methanol, and HF. *J. Chem. Phys.* **2000**, *113*, 9113−9121.
(40) Shih, J.; Sheu, S.; Mou, C. A Voronoi Polyhedra Analysis of Structures of Liquid Water. *J. Chem. Phys.* **1994**, *100*, 2202−2212.
(41) Medvedev, N. N.; Voloshin, V. P.; Luchnikov, V. A.; Gavrilova, M. L. An Algorithm for Three-dimensional Voronoi S-network. *J. Comput. Chem.* **2006**, *27*, 1676−1692.
(42) The VNP code. http://www.kinetics.nsc.ru/mds/?Software:VNP, Accessed: 05-07-2016.
(43) Voloshin, V. P.; Medvedev, N. N.; Andrews, M. N.; Burri, R. R.; Winter, A. Roland Geiger Volumetric Properties of Hydrated Peptides: Voronoi-Delaunay Analysis of Molecular Simulation Runs. *J. Phys. Chem. B* **2011**, *115*, 14217−14228.
(44) Voloshin, V. P.; Kim, A. V.; Medvedev, N. N.; Winter, A. Roland Geiger Calculation of the Volumetric Characteristics of Biomacromolecules in Solution by the Voronoi-Delaunay technique. *Biophys. Chem.* **2014**, *192*, 1−9.
(45) Sosso, G. C.; Miceli, G.; Caravati, S.; Giberti, F.; Behler, J.; Bernasconi, M. Fast Crystallization of the Phase Change Compound GeTe by Large-Scale Molecular Dynamics Simulations. *J. Phys. Chem. Lett.* **2013**, *4*, 4241−4246.
(46) Hassanali, A. A.; Giberti, F.; Sosso, G. C.; Parrinello, M. The Role of the Umbrella Inversion Mode in Proton Diffusion. *Chem. Phys. Lett.* **2014**, *599*, 133−138.
(47) An α shape associated with a set of points is the generalization of the concept of convex hull (see, e.g., ref 56).
(48) *MATLAB*, version 7.10.0 (R2010a); The MathWorks Inc.: Natick, MA, 2010.
(49) Ruocco, G.; Sampoli, M.; Vallauri, R. Analysis of the Network Topology in Liquid Water and Hydrogen Sulphide by Computer Simulation. *J. Chem. Phys.* **1992**, *96*, 6167−6176.
(50) Godawat, R.; Jamadagni, S. N.; Garde, S. Characterizing hydrophobicity of Interfaces by Using Cavity Formation, Solute Binding, and Water Correlations. *Proc. Natl. Acad. Sci. U. S. A.* **2009**, *106*, 15119−15124.
(51) Garde, S.; Hummer, G.; Garcia, A. E.; Paulaitis, M. E.; Pratt, L. R. Origin of Entropy Convergence in Hydrophobic Hydration and Protein Folding. *Phys. Rev. Lett.* **1996**, *77*, 4966.
(52) Vaikuntanathan, S.; Rotskoff, G.; Hudson, A.; Geissler, P. L. Necessity of Capillary Modes in a Minimal Model of Nanoscale Hydrophobic Solvation. *Proc. Natl. Acad. Sci. U. S. A.* **2016**, *113*, E2224−E2230.
(53) Hassanali, A.; Giberti, F.; Cuny, J.; Kühne, T. D.; Parrinello, M. Proton Transfer Through the Water Gossamer. *Proc. Natl. Acad. Sci. U. S. A.* **2013**, *110*, 13723−13728.
(54) Gibb, C. L. D.; Gibb, B. C. Anion Binding to Hydrophobic Concavity Is Central to the Salting-in Effects of Hofmeister Chaotropes. *J. Am. Chem. Soc.* **2011**, *133*, 7344−7347.
(55) Thompson, J.; Soni, B.; Weatherill, N. *Handbook of grid generation*; CRC Press: Boca Raton: London, 1999.
(56) Skiena, S. *The algorithm design manual*; TELOS - The Electronic Library of Science: Santa Clara, CA, 1998.

DOI: 10.1021/acs.jpca.6b11168
J. Phys. Chem. A 2017, 121, 370−380